

63-3-1

CATALOGED BY ASTIA
AD No. 400109

INVESTIGATION OF MICROWAVE NON-LINEAR
EFFECTS UTILIZING FERROMAGNETIC MATERIALS

THIRD QUARTERLY PROGRESS REPORT
Period September 17 to December 16, 1962

400109

Melabs

**research
development
manufacture**

Work performed for the U.S. Army Signal
Research and Development Laboratory
Fort Monmouth, New Jersey
under Contract
No. DA 36-039 SC-89206

ASTIA
RECEIVED
APR 8 1963
ASTIA



INVESTIGATION OF MICROWAVE
NON-LINEAR EFFECTS UTILIZING FERROMAGNETIC MATERIALS

THIRD QUARTERLY PROGRESS REPORT
Period September 17, 1962 to December 16, 1962

The objective of this research and development program is to investigate the non-linear effects in the microwave properties of ferrites and ferromagnetic garnet materials.

Work performed under Signal Corps Contract No.
DA 36-039 SC-89206

Report prepared by:


Roy W. Roberts

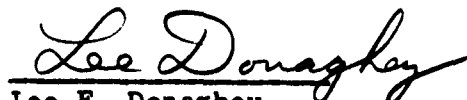

Lee F. Donaghey

TABLE OF CONTENTS

<u>Section</u>		<u>Page</u>
I	PURPOSE	1
II	ABSTRACT	1
III	PUBLICATIONS, LECTURES, REPORTS AND CONFERENCES	2
IV	FACTUAL DATA	3
	A. Introduction	3
	B. Theoretical	3
	C. Experimental Data	11
V	CONCLUSIONS	30
VI	PROGRAM FOR NEXT QUARTER	31
VII	IDENTIFICATION OF PERSONNEL	32

LIST OF FIGURES

<u>Figure No.</u>		<u>Page</u>
1	Resonance frequency versus sample dimensions in a dielectric center for the cylinder placed between parallel conducting plates.	13
2	Resonance frequencies as a function of length, L, and diameter, D, of a dielectric cylinder containing a 0.079" diameter YIG sphere, showing possible frequency wave families.	13
3.	Pump frequency-range mode plot for a 0.079" diameter YIG sphere at the geometric center of a .123" diameter by .168" length Stycast K-15 cylinder.	14
4.	Guided half-wavelengths versus frequency for the TE_{11} , TM_{011} and TE_{01} modes in a cylindrical guide of 0.500" diameter.	16
5.	Tuning curves for dielectric cylinders: resonance frequency versus tuning parameter, d.	20
6.	Dielectric cylinder resonances observed in a .175" length, .180" diameter cylinder as a function of tuning parameter, d.	21
7.	Magnetodynamic mode plot for a .1685" length dielectric cylinder containing a 0.70" diameter YIG sphere, as a function of cylinder diameter.	23
		25

I. PURPOSE

This research and development program shall investigate the non-linear effects in the microwave properties of ferrites and ferrimagnetic garnet materials. Principal emphasis will be placed on determining the feasibility of and parameters for efficient ferrite parametric amplification. In addition, the sources of noise will be investigated for dependence on design parameters.

II. ABSTRACT

A method of comparing the relative threshold pump fields necessary for sustaining longitudinally pumped parametric amplification for various signal and idle magnetodynamic mode pairs and Q's is derived from the threshold pump field expression. Selection rules are obtained for transverse electromagnetic field coupling of dielectric to static modes in a dielectric cylinder containing a spherical YIG sample. Amplifier operating parameters are explored by considering selection rules governing strong dielectric to static mode coupling. Resonance mode densities were obtained experimentally in the signal frequency band. Pump energy resonance was investigated, and a method for frequency tuning of magnetodynamic signal mode was explored. Cavity resonance of the pump in the TE_{102} mode was used for pumping in several coupled-guide amplifier configurations; experiments were hampered by pump power difficulties. Data on transient pumping characteristics is presented.

III. PUBLICATIONS, LECTURES, REPORTS AND CONFERENCES

On October 29 and 30, 1962, Mr. Roy W. Roberts visited USASRDL to discuss contract progress and technical information with Mr. Sam Dixon, Dr. Martin Auer, and Mr. John Carter.

IV. FACTUAL DATA

A. Introduction

Under the present contract, the magnetodynamic mode of operation of a ferrite parametric amplifier is under investigation. The magnetodynamic ferrite resonance modes are mixed magnetic-cavity resonances resulting from coupling of shape-dependent magnetostatic resonances with volume-dependent electromagnetic resonances in large ferrimagnetic samples. Objectives of the contract are the design and operation of a low pump power and low noise level amplifier. Magnetodynamic mode operation may allow reduction of both pump power required and noise figure over that of other modes of ferrite amplifier operation due to operation in a frequency-field region where the density of spurious modes is small.

B. Theoretical

1. An expression for the threshold pump fields necessary for sustainment of longitudinally pumped parametric amplification was obtained in a previous report¹ by evaluating the negative resistance which one tuned circuit reflects into another through parametric coupling. The form of the pump field expression given is as follows:

$$h_p = A_p \epsilon^{i\theta_p} \mathcal{H}_p \quad (1)$$

where \mathcal{H}_p is a dimensionless distribution function.

¹ R. Roberts, "Investigation of Microwave Non-Linear Effects Utilizing Ferromagnetic Materials" Research Contract DA36-039 SC-87412, Final Report, October 31, 1960, p. 114

The coefficient, A_p , is given by the expression

$$A_p = \frac{M_0}{2F\sqrt{Q_s Q_i}} \quad (2)$$

where M_0 is the magnetization within the ferrite, F is the filling factor, and Q_s and Q_i are the signal and idle mode Q 's. F may be expressed in terms of an integral over the magnetization product for signal and idle, as follows:

$$F = \left| \mu_0 \int_{\text{ferrite}} e^{i\theta_p} H_p \vec{m}_s \cdot \vec{m}_i dv \right| k' \quad (3)$$

where the coefficient k' is a proportionality constant whose magnitude is a function of losses in the system.

Combining (2) and (3) into (1) obtains the threshold pump field expression,

$$h_p = \frac{k e^{i\theta_p} H_p}{\sqrt{Q_s Q_i} \left| \int_{\text{ferrite}} e^{i\theta_p} H_p \vec{m}_s \cdot \vec{m}_i dv \right|} \quad (4)$$

The above expression allows calculation of the threshold pump fields for an arbitrary choice of magnetodynamic modes to within a multiplicative constant. The optimum choice of amplifier modes allowing minimum pump power may then be determined, independent of the magnitude of losses in the system, by solving for the loaded Q product and magnetization overlap integral as a function

of magnetodynamic mode pair, and dc magnetic bias field-frequency conditions. Once the optimum field-frequency conditions and mode pair are selected, the pump field threshold may be reduced by lowering the losses due to fabrication techniques and to choice of materials used in the amplifier construction.

Consider a dielectric resonator containing a sample of ferrite material of arbitrary size and shape. An externally applied dc magnetic field, \hat{H}_0 , is applied parallel to the pumping fields \vec{h}_p at frequency ω_p , so as to produce a magnetization within the sample. As the theoretical threshold pump power, $(P_p)_{th}$, is inversely proportional to the signal and idle Q product, the dependence of $(P_p)_{th}$ on the form of the magnetodynamic modes may be qualitatively investigated by obtaining expressions for the loaded Q's of the magnetodynamic modes. Let ω_m , Q_m and ω_c , Q_c be the frequencies and Q's of static and cavity resonance modes respectively. Then for the simplified system of one cavity and one static mode, a set of coupling equations may be written as follows:

$$\begin{aligned} [\omega - \omega_m (1 + j/2Q_m)] A_m + K_{mc} A_c &= 0 \\ [\omega - \omega_c (1 + j/2Q_c)] A_c + K_{cm} A_m &= 0 \end{aligned}$$

(5)

where A_c , A_m are the amplitudes of the cavity and static fields, and K_{mc} and K_{cm} are coupling coefficients. Equations

(5) have a solution when the determinant of the coefficients is set equal to zero, whence

$$\omega_{1,2} = \frac{1}{2} \left[\omega_m + \omega_c + \frac{1}{4} \left(\frac{1}{Q_m} + \frac{1}{Q_c} \right) \pm \sqrt{(\omega_m - \omega_c)^2 - \left(\frac{\omega_m}{2Q_m} - \frac{\omega_c}{2Q_c} \right)^2 + k_{mc} k_{cm} + j(\omega_m - \omega_c) \left(\frac{\omega_m}{2Q_m} - \frac{\omega_c}{2Q_c} \right)} \right] \quad (6)$$

In equation (6) the square-root term represents a measure of the splitting of the coupled modes away from their decoupled values, whereas the imaginary term is a measure of the coupled Q of the system.

Finally, by expanding the square-root term in equation (6) the coupled Q of the system, from $\text{Im}(\omega) = \frac{\omega'}{2Q}$, becomes,

$$Q_{1,2} \approx \frac{1}{2} \left\{ \frac{\omega_m + \omega_c \pm \sqrt{(\omega_m - \omega_c)^2 - \left(\frac{\omega_m}{2Q_m} - \frac{\omega_c}{2Q_c} \right)^2 + 4k_{mc} k_{cm}}}{\frac{\omega_m}{2Q_m} + \frac{\omega_c}{2Q_c} \pm \frac{(\omega_m - \omega_c) \left(\frac{\omega_m}{2Q_m} - \frac{\omega_c}{2Q_c} \right)}{\sqrt{(\omega_m - \omega_c)^2 - \left(\frac{\omega_m}{2Q_m} - \frac{\omega_c}{2Q_c} \right)^2 + 4k_{mc} k_{cm}}}} \right\} \quad (7)$$

Equation (7) shows that $Q_{1,2}$ increases to Q_c for increasing

$|\omega_m - \omega_c|$ and $K_m c K_{cm}$ for one magnetodynamic mode branch, and decreases to Q_m for the other.

The physical system is complicated by the presence of other resonances which participate in the splitting phenomena; the above approximations still may be used, where the density of additional resonances is low, to allow relative Q measures of various working points of the parametric amplifier along the magnetodynamic modes.

The magnetization overlap integral $\int_{\text{ferrite}} \epsilon^{i\theta_p} H_p \vec{m}_i \cdot \vec{m}_i dv$

may be calculated from expressions of estimates on the pump field distribution, H_p , and on the magnetization functions, m_i within the sample. When the dielectric cylinder is placed in a region of uniform pump fields, the function H_p may be considered to be unity throughout the sample, and does not enter into the overlap integral.

Mode designation for resonances in the dielectric cylinder were given in a previous report.² The types considered are the $TE_{on\ell}$, $TM_{on\ell}$, $HE_{mn\ell}$, and $EH_{mn\ell}$, where the azimuthal functional dependence takes the form $\epsilon^{\pm im\phi}$, the radial functional

² R. Roberts, "Investigation of Microwave Non-Linear Effects Utilizing Ferromagnetic Materials" Research Contract DA36-039 SC-89206, Second Quarterly Report, September 16, 1962.

dependence is as $A J_m'(\rho) + B J_m(\rho)$ where $\rho^2 = [k^2 - (2\pi/L)^2] r^2$ and the axial functional dependence is of the form $\frac{\sin}{\cos} \left\{ (2\pi/L)(z - L/2) \right\}$.

Magnetostatic modes, as presented by Fletcher and Bell³, may be given the designation MS_{nmr} where n is the orbital, m the azimuthal, and r the radial variable, and have a potential function of the form

$$\psi \sim r^{-n-1} P_n^m(\cos\theta) = (1-z^2)^{-n-1} f_n^m(z^2) g(z) \quad (8)$$

where $g(z)$ is z for $n+m$ odd, and 1 for $n+m$ even.

Also, $z = \cos\theta$ and $|m| \leq n$. The magnetic field intensities may be obtained from the potential function by the expressions

$$\begin{aligned} 4\pi m_x &= K \frac{\partial \psi}{\partial x} - i\nu \frac{\partial \psi}{\partial y} \\ 4\pi m_y &= i\nu \frac{\partial \psi}{\partial x} + K \frac{\partial \psi}{\partial y} \end{aligned} \quad (9)$$

where $K = \Omega_H / (\Omega_H^2 - \Omega^2)$
 $\nu = \Omega / (\Omega_H^2 - \Omega^2)$
and $\Omega = \omega / 4\pi\gamma M_0$
 $\Omega_H = H_i / 4\pi M_0$.

In the terminology of Fletcher, the magnetic bias field, increases as r goes from 1 to zero. Magnetization values, $4\pi m_x$ and $4\pi m_y$ are given by Fletcher and Solt, as functions of the permeability tensor components, K and ν , and may be reduced to spatial amplitude functions for chosen frequency and $4\pi M_s$ of

3. P.C. Fletcher and R.O. Bell, "Ferrimagnetic Resonance Modes in Spheres", Hughes Aircraft Company, Culver City, California, unpublished.

the ferrimagnetic material.

For the MS₃₁₀ mode, for example, letting $4\pi M_s = 1750 \text{ Oe}$,
 $f_p = 34.6$, $f_s = 17.3 \text{ kmc}$ gives:

$$\Omega_H = H_c / 4\pi M = 2.98$$

$$\Omega = \omega_{310} / \gamma 4\pi M = 3.209$$

$$K = -2.10$$

$$\nu = -2.25$$

and

$$\begin{aligned} 4\pi m_x &= \frac{1}{a^3} \{ 199z^2 - 0.45x^2 + 0.55y^2 - 1.11ixy + 26a^2 \} \\ 4\pi m_y &= \frac{1}{a^3} \{ 199z^2 + 0.55x^2 - 0.45y^2 + 1.11ixy + 26a^2 \} \end{aligned} \quad (10)$$

the signal-idle magnetization overlap integral may be computed from the above technique, however, only for large splitting factors and near the Walker spectrum, so that the magnetization vector of the magnetodynamic modes may be approximated by that for magnetostatic modes. Once the magnetization components are computed for other modes, particularly the 110, 311, $\bar{3}\bar{1}1$, and $5\bar{1}1$, the signal-overlap integral may be obtained for pairs of these modes, and the results used to allow comparison of the pump field threshold for various working points of the amplifier on magnetodynamic modes, when combined with measures of Q.

2. Selection rules may be obtained for transverse electromagnetic field coupling of dielectric to static modes. The method employs expressions for short circuited boundary conditions, and leads to a designation of optimum eigenvalue dependence of signal, idle and pump modes.

For dc magnetic bias field along the axis of the dielectric cylinder:

$$\begin{aligned}
 (\vec{m}_z)_{\text{pump}} &= \frac{1}{2} (\vec{m}_t)_{\text{signal}} \cdot (\vec{m}_t)_{\text{idle}} \hat{z} \\
 &\sim e^{i(m_s + m_i)d} \\
 (h_{c_z})_{\text{pump}} &\sim e^{i m_p d}
 \end{aligned}
 \tag{11}$$

The integral representation of pump power vanishes unless:

$$\begin{aligned}
 m_p - m_s - m_i &= 0 \\
 P_{\text{pump}} &= i \left(\frac{\omega_p}{2} \right) \int_{\text{ferrite}} h_c \cdot (\vec{m}_z)_p^* dv \\
 &\sim \int_{\text{ferrite}} \left(\frac{\omega_p}{2} \right) \int e^{j(m_p - m_s - m_i)d}
 \end{aligned}
 \tag{12}$$

For $m_p = 0$ the selection rule becomes $m_s + m_i = 0$ and the TE_{odd} may be used for pumping.

Short circuited boundary conditions at the ends of the dielectric cylinder give the equality:

$$\begin{aligned}
 h_{c_z}(r, d, -z) &= (-1)^l h_{c_z}(r, d, z) \\
 [m_t(r, d, -z)_{\text{sig}}] [m_t(r, d, -z)_{\text{idle}}] &= (-1)^{m_s + m_i + n_r + m_i} [m_t(r, d, z)_{\text{sig}}] [m_t(r, d, z)_{\text{idle}}]
 \end{aligned}
 \tag{13}$$

Again, the integral representation for pump power absorbed vanishes unless

$$m_s + n_s + n_i + m_i = l_p, \text{ even.}$$

These general conditions, $m_p = m_s + m_i$ and $m_s + n_s + n_i + m_i$, even, may be reduced by allowing $m_p = l_p = 0$ where upon the selection rules are reduced to those given in the last quarterly report. Pump modes where m_p and l_p are different than zero are important only when the dielectric cylinder is resonant to the pump mode; i.e., when the cylinder is used as a resonator for pump fields. Such resonance of the pump is desirable because of increased filling factor and tight coupling over that allowed by cavity resonance of the pump; disadvantages are the lowering of pump circuit Q due to the relatively high losses in the dielectric, and to tunability limitations where a relatively fixed pump frequency is available.

C. Experimental Data

1. Resonance mode densities were obtained experimentally for a dielectric cylinder containing a .118" diameter YIG sphere at its geometric center. Loading of the cylinder modes was achieved by means of a slot inductive iris placed in an adjacent conducting plate. The use of such an iris allowed resonance of only those modes which have magnetic fields at the end of the cylinder in the direction of the iris slot. Such modes are the proposed HE_{112} signal mode, and others into which the HE_{112} could readily couple. Cylinder diameters larger than

required were chosen so as to bring resonance frequencies into the frequency range of the p-band sweep generator.

Samples were prepared by machining pairs of stycast K-15 cylinders of uniform diameters and parallel end faces. Into one end of each cylinder of a pair, a semi-spherical cavity was cut so as to allow imbedding of the .118" DIA YIG sphere. Cylinder ends are joined to contain the sphere, and length is finally machined to leave the sphere at the geometric center. Cylinders of .150", .180", .200" and .250" diameter were chosen, and resonance frequencies versus length obtained by decreasing the length by machining, between measurements. An inductive taper was prepared in k-band guide of length, 2", reducing the height of the guide from .170" to .030". The tapered end was brazed to a plate so as to allow a .420" by .030" iris in the plate face. Measurements of resonant frequencies were made by placing a second, parallel plate against the other end of the cylinder. Resonance absorption was observed in reflected power from a p-band, 12 to 18 Kmc generator. The absorptions due to resonance could be distinguished from those due to VSWR by placing the sample and iris assembly into the field of a Varian magnet, and observing detuning of resonance frequency with change in the magnetic field applied.

Resonance frequency as a function of cylinder dimension is shown in Figure 1. The shape of the curves is expected to

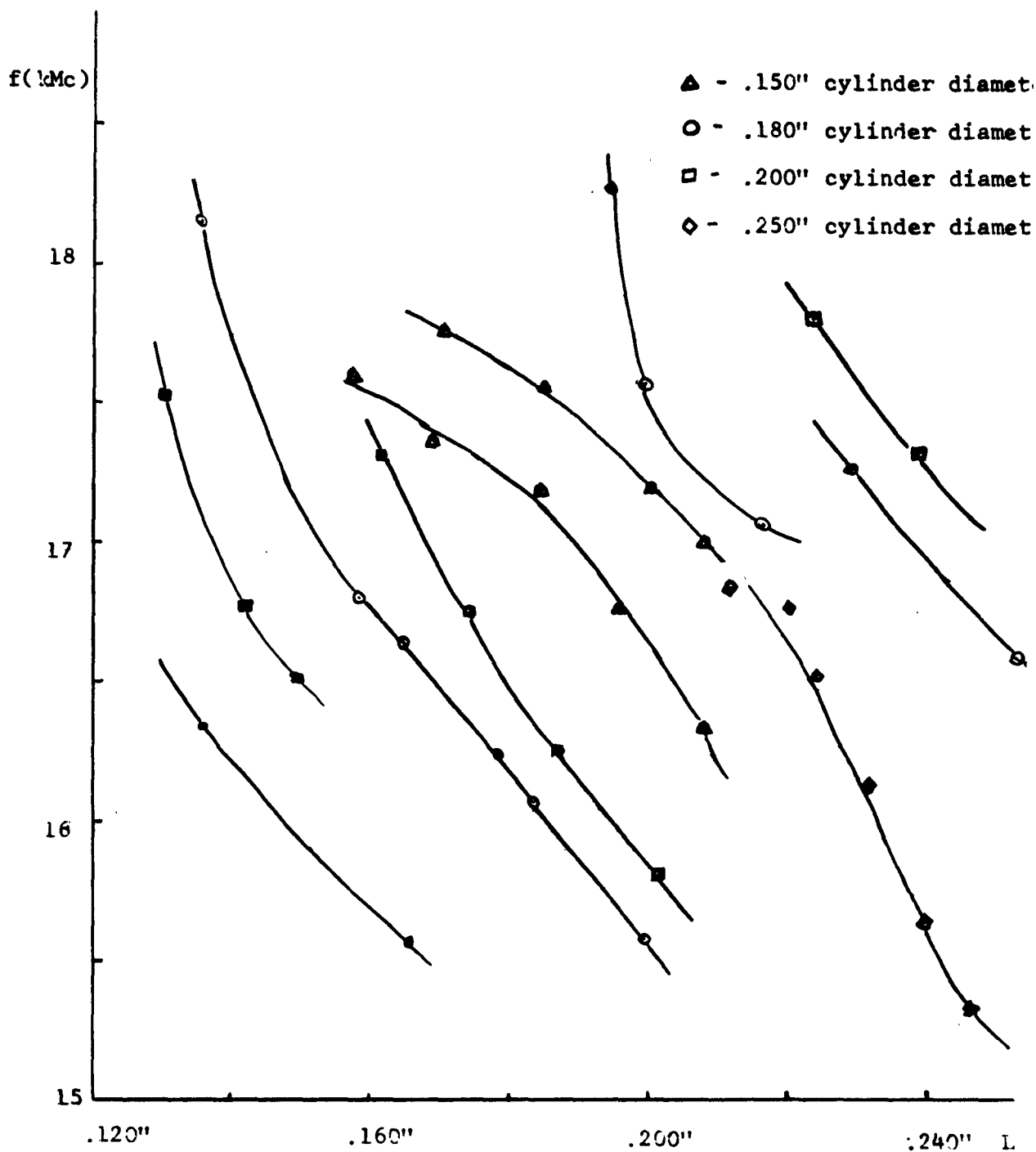


FIGURE 1

Resonance frequency versus sample dimensions in a dielectric cylinder loaded with a .118" diameter YIG sphere at the geometric center, for the cylinder placed between parallel conducting plates, and loaded by means of an iris at one end of the cylinder.

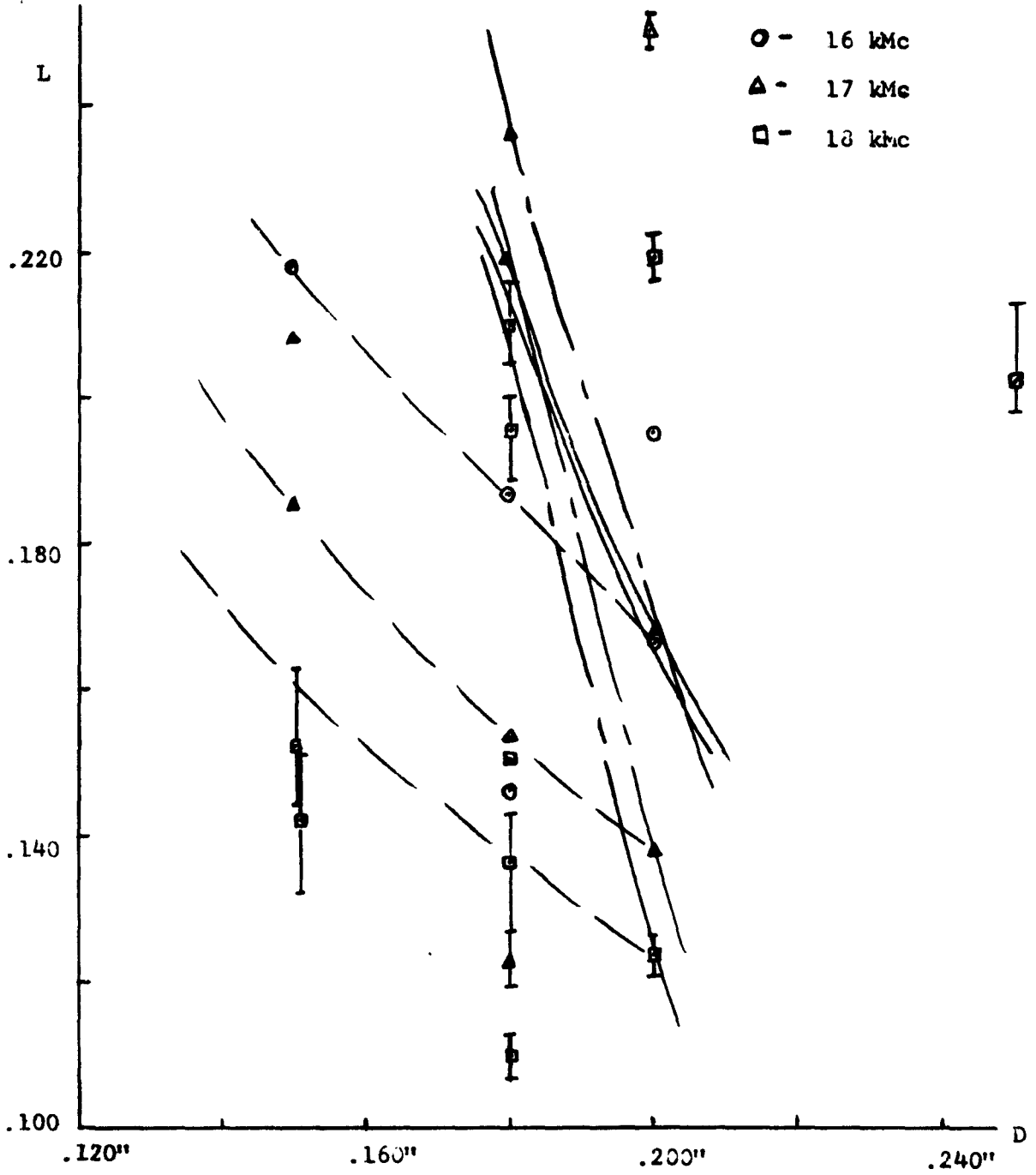


FIGURE 2

Resonance frequencies as a function of length, L, and diameter, D, of a dielectric cylinder containing a .079" diameter YIG sphere, showing possible frequency curve families.

be convex toward the origin for cylinder resonances, and as such, the curvature of resonances for the 0.150" DIA cylinder is not consistent, and may be due to frequency detuning by a spherical resonance in the YIG sphere.

A length versus diameter plot may be obtained from Figure 1 by finding the intersections of the curves obtained with a constant frequency line, obtaining Figure 2. It was hoped that the data so obtained would lead to the identification of other modes present in the cylinder, and two such modes are shown. Additional data should lead to the experimental determination of the complete set of resonances for a cylinder of arbitrary size. Such an investigation is of low priority at the present time, however.

2. Pump-cavity resonances and magnetodynamic modes were investigated in a .123" diameter cylinder .168" long containing a .079" diameter YIG sphere at the geometric center in order to explore the possibility of resonating the pump in the cylinder. Reflected signal from a p-band sweep generator was monitored for various amplitudes of the applied dc magnetic field. The cylinder was placed between parallel conducting plates, and coupling to waveguide was achieved by means of an inductive iris in one plate, adjacent to a cylinder end wall. Data obtained is shown in Figure 3.

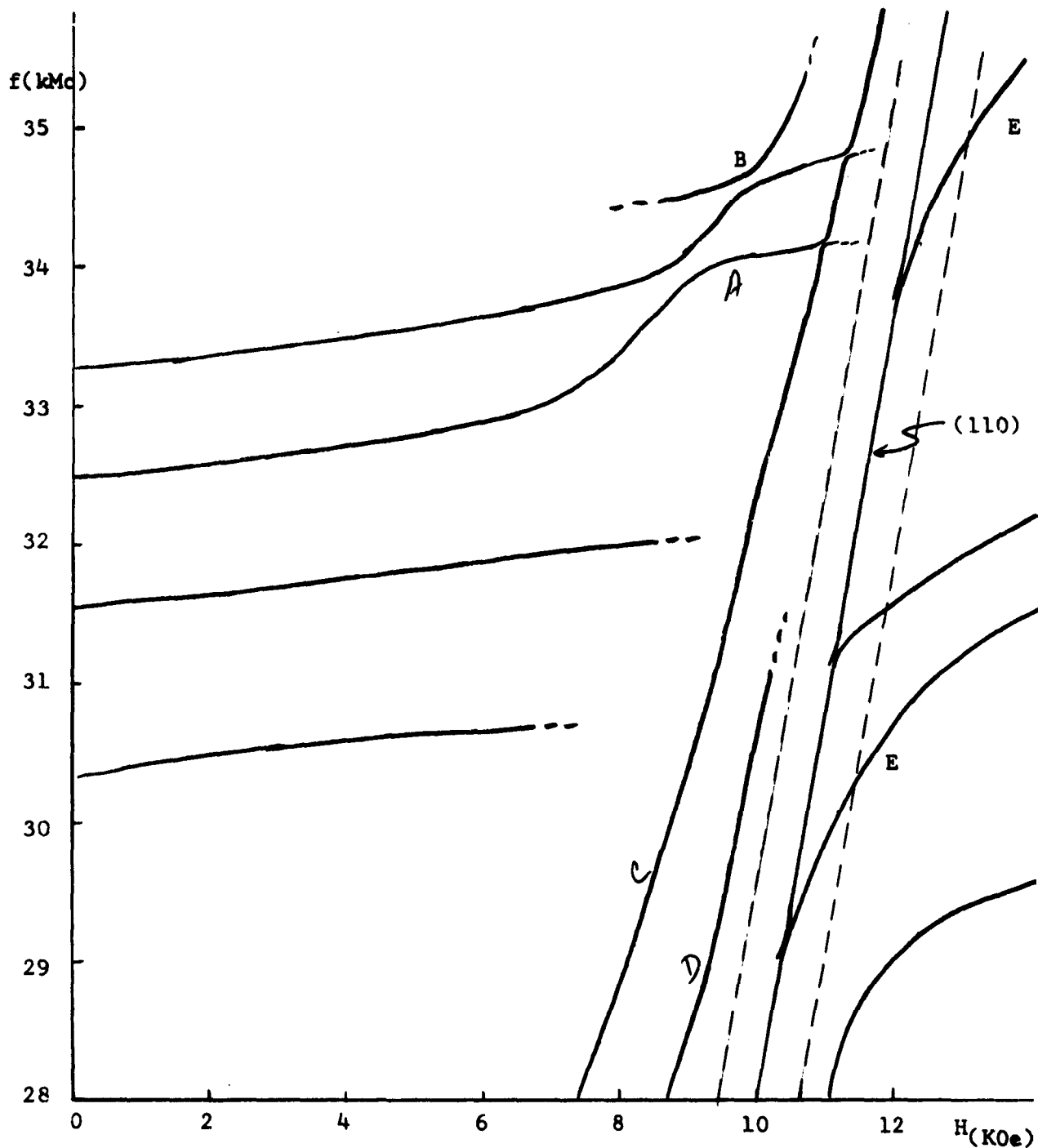


FIGURE 3

Pump frequency range mode plot for a .079" diameter YIG sphere at the geometric center of a .123" diameter by .168" length stycast K-15 cylinder.

Figure 3 shows several magnetostatic modes detuned by cavity resonances. The magnetodynamic modes so obtained were found to be describable by either very large or very small splitting factors. Mode branches marked "C" and "D" may be described by a large splitting factor, and others by a small splitting factor for magnetodynamic mode branches below precessional resonance fields. Magnetodynamic mode branches for above-precessional resonance fields were found to have large splitting factors, and seemed to couple to the uniform precession, as well as other unidentified modes. The degree of splitting depends on the degree of coupling between the spin system of a certain magnetostatic mode, and the cavity resonance mode, so that variable splitting factors for different magnetodynamic mode branches is expected.

Of note is the splitting of one magnetodynamic mode with another, indicated by points A and B. Here, the magnetodynamic mode marked "C" shows strong coupling between a cavity resonance and a static mode, and weaker coupling to two other magnetodynamic modes. The coupling between magnetodynamic modes may be due to a magnetodynamic mode occurring for higher resonance frequency. As both points A and B lie outside the Walker mode manifold, it may be possible to amplify at low pump powers at these points without pumping other unwanted spin waves to instability.

Pumping at points E on magnetodynamic modes on the high field side of the Walker spectrum allows a favorable reduction in noise, by lowering the pump frequency required below that required for degenerate operation, as pointed out in the first quarterly for the present contract. The magnetodynamic modal branches recorded on the high-field side of the Walker spectrum, however, all seem to couple most strongly with the uniform precessional 110 mode, rather than with the 310 or 210 which lie closer to the high-field boundary of the Walker spectrum and which were thought to be most readily detuned outside the spectrum. Such is not surprising, as the predominant energy of the spin system is present in the uniform precessional, or 110 mode; under detuning by cavity resonance, the spin mode becomes mixed to some degree due to other ferrite modes, but most of the spin energy remains in the detuned 110 mode. Thus, for amplifier operation on the high-field magnetodynamic branches, the detuned 511 may be used as an idle when the 110 is used as a signal mode.

3. Signal tuning of magnetodynamic modes was investigated using a cylindrical plunger and guide mounted on the broad wall of the k-band signal guide. The cylindrical/guide consisted of a brass tube brazed perpendicular to the broad wall of the signal guide, containing a rod-plunger which could be brought into proximal contact with one end of the dielectric cylinder placed in the signal guide. A p-band sweep generator was employed as signal, and either transmitted or reflected power was

monitored. A doubler was used in conjunction with the sweep generator to investigate tuning at pump frequencies. The diameter of the cylindrical guide was chosen to be 0.500" so as to allow propagation of the TE_{11} mode for frequencies above 14.85 kMc, and of the TE_{01} above 28.75 kMc. Signals resonating in the dielectric cylinder would then be expected to be launched from the end of the dielectric, and be tunable in frequency by the plunger in the cylindrical guide. The resonances at a particular frequency should appear at a sequence of plunger positions determined by the guided wavelength of a particular mode within the cylindrical guide and thus lead to a determination of the orbital type of each dielectric cylinder mode investigated in the tuning apparatus. Guided half-wavelengths of various modes are shown in Figure 4.

Tuning curves for cylinders of .174", .138", .1225" and .105" diameters and length .1685" containing a .079" diameter YIG sphere and data therefrom is shown in Figure 5. Tuning distance, d , was measured as the distance between the tuning plunger and the dielectric cylinder end. The tuning curves show a decrease in resonant frequency (at $d=0$) for increasing dielectric cylinder diameter in the same dielectric mode. Slope of the curves is discontinuous, however, and is not readily explained. No other resonances than those shown were observed for the dielectric cylinders indicated.

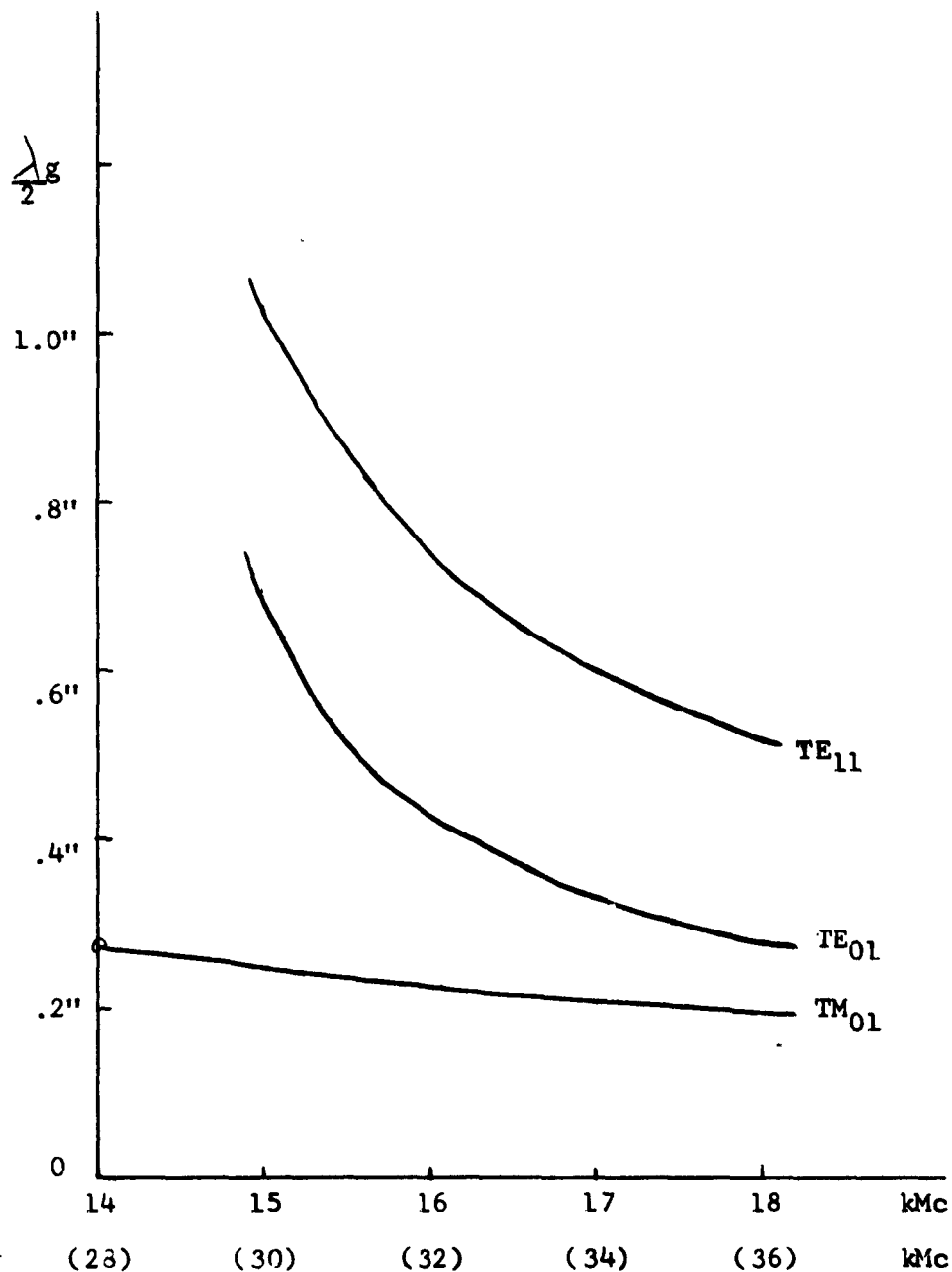


FIGURE 4

Guided half-wavelengths versus frequency for the TE₁₁, TM₀₁, and TE₀₁ modes in a cylindrical guide of 0.500" diameter.

f (kMc)

21

20

19

18

17

16

15

14

- ◇ - .105" cylinder diameter
- - .1225" " "
- - .138" " "
- △ - .174" " "

0 .2" .4" .6" .8" 1.0" d

FIGURE 5

Tuning curves for dielectric cylinders:
resonance frequency versus tuning parameter, d.

Tuning was investigated in dielectric cylinders of larger dimension in which several modes could be sustained in resonance. Tuning curves are shown in Figure 6. Several effects may be noted: First, VSWR spikes were found to change frequency rapidly with increased, d ; the effect is present only for d near zero, and is due to distortion of standing waves at the crystal detector. Second, some dielectric cylinder resonances were found to be insensitive to d for large d . The resonant frequency change due to removing one end plate was always found to be negative, and less than one kMc at p-band. Third, the introduction of an iris at one end of the cylinder decreased the resonance frequency. The resonances observed to be tuned only for d near zero; i.e., only when the metal wall is near the cylinder end, may be the true dielectric resonance, whereas those tunable overall may be resonances associated with the cylindrical tuning guide in which the tuning plunger is mounted.

In order to achieve signal tuning which does not substantially distort the pump fields, it is necessary for d to be restricted to small values. Such a restriction, however, may not be a disadvantage, as signal tuning is most effective for small values of d ; proper tuning devices will require that VSWR effects be minimized.

4. Variation in magnetodynamic mode position in frequency-field coordinates was investigated for a cylinder of

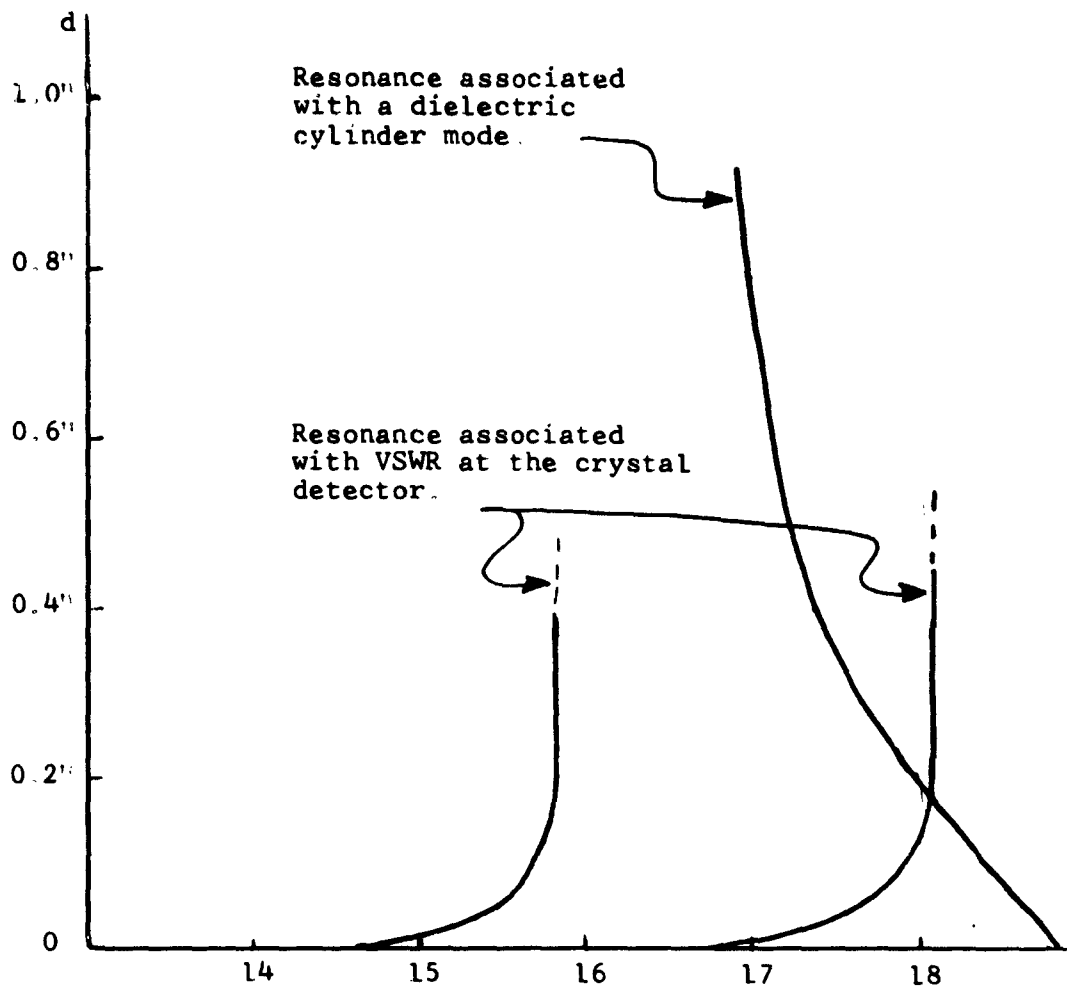


FIGURE 6

Dielectric cylinder resonances observed in a .175" length, .180" diameter cylinder as a function of tuning parameter, d . Note that two resonances are tunable only for d near zero.

length .1685" and diameters 0.105", .1225", and .138" containing the .079" diameter YIG sphere. The frequency at which the magnetodynamic mode is observed to cross the high field boundary of the Walker spectrum decreases with increasing cylinder diameter. The length and diameters chosen are appropriate for sustaining the HE_{112} electromagnetic dielectric mode. The results are shown in Figure 7.

5. Cavity resonance of pump energies in the TE_{102} mode was investigated initially for several waveguide configurations. In each, the YIG loaded dielectric cylinder was placed at the geometric center of the rectangular pump cavity, and signal power was coupled into the cylinder by means of an inductive iris in the broadwall of the cavity and adjacent to the cylinder with k-band signal guide meeting the iris oriented so as to minimize coupling of pump energies into the signal guide. The dc magnetic field was applied transverse to the pump waveguide so as to allow parallel pumping. Reflected signal power from a p-band sweeper was monitored.

Interaction was obtained for a .140" DIA cylinder containing a .118" DIA YIG sphere and for a pump frequency of 35.66 kMc. The interaction appeared to be constrained oscillation at a frequency, field-tunable, between 17.7 and 18 kMc. The oscillation amplitude was found to be independent of pump power for large values of pump power, and to decrease rapidly

with decreasing pump power below an unmeasured threshold. Amplification data was not obtained when experiments were continued due to failing pump power and stability of the output pulse of the MA201-B magnetron.

Interaction in the frequency range from 22 to 26 kMc was obtained for a .126" diameter cylinder of .168" length containing a .118" DIA YIG sphere, for the cylinder inserted into the pump guide so that the cylinder side lay against the signal iris. The interactions were found to be extremely dependent on dc magnetic field, and may represent precessional resonance at appropriate magnetic fields. No unconstrained oscillation was identified. The pump power was measured shortly after the above experiments, and was found to be nine watts peak, possibly too low for sustaining amplification with the low pump Q of the above system.

6. Pump Power Difficulties: The two pump power supplies available at k-band for application to the parametric amplifier have been the Elliott 8TFK2 klystron, and the Microwave Associates 201-B magnetron.

The Elliott klystron is a continuous wave tube, and tunable over the frequency interval from 32.17 to 36.10 kMc. Output power is between 20 and 31 watts on the frequency interval from 33.3 to 36.1 kMc. The tube was incorporated into the

microwave circuit during the second week of this quarter, and, during preliminary set-up tests, failed by opening of the filament. The tube was returned to Litton Industries, the Elliott supplier, and finally to England for repairs. It was reported in early December that no apparent cause of failure could be determined, and that the tube could be repaired at nominal cost. The tube should again be available for use with the parametric amplifier early in January, 1963.

During the quarter, a fixed frequency Elliott 8FK1 klystron operable with 16.5 watts at 34.725 kMc was obtained on loan from Litton Industries. The tube was found to be deficient in collector current with the same power supply used with the Elliott 8TFK2 klystron. The power supply was thoroughly checked for the required outputs, and meters calibrated. Again the tube did not oscillate and drew low collector current. It was assumed that the focussing structure was out of alignment, and as the tube could not be used, the tube was returned to Litton Industries for repairs.

Use of the continuous wave Elliott klystrons is preferred to that of the presently owned Microwave Associates 201-B Magnetron due to the stability of the former tube, and to the failing output power obtainable from the latter. Also, several advantages obtain from continuous wave pumping, such as elimination of transient pumping characteristics occurring at turn-on as

well as turn-off of the pump, and ease in visually observing the parametric interactions.

The Microwave Associates 201-B magnetron is a tunable pulsed tube on the frequency interval from 34.6 to 35.1 kMc with output ratings of 35 KW with a .0004 duty cycle. The present tube, however, due to its extended age, does not have the above characteristics, but has a fixed 35.66 and 34.8 kMc bi-mode frequency. Power measurements showed the tube to operate on a two microsecond pulse with 750 watts peak in May with 410 watts in September, 1962.

The modulator was reconditioned to allow a two microsecond pulse, although the modulator contribution to pulse instability was not completely removed, and the pulse amplitude was found to vary with time throughout the pulse period. At the conclusion of tests in mid-December, the magnetron power output was again measured and found to be 9 watts-peak stable, and 15 watts-peak unstable. The frequency of stable operation was found to have shifted to 35.68 kMc.

7. Transient Pumping Characteristics: The amplitude of oscillations recorded were found to be time dependent throughout the duration of the pulse. First, for constant pump power, and as the applied dc magnetic field is increased through resonance, the point of maximum interaction amplitude remains constant in

time with respect to the pumping pulse, and the maximum value varies as a Lorentz-linewidth about the resonance dc field value. The interaction amplitude rises steeply to maximum at the end of the two microsecond pulse, and is small during the first microsecond.

Secondly, for constant dc field and decreasing pump power, the maximum interaction amplitude remains at the end of the pumping pulse.

Measurements were made at p-band frequencies with a YIG sphere imbedded in a dielectric cylinder and placed in a TE_{102} cavity. Signal fields reached the cylinder through an iris slot in the broad wall of the cavity, and reflected power was monitored.

The findings suggest that information regarding the pump is being lost by the short duration of the presently available pulse, preventing a complete display of transient resonance response.

V. CONCLUSIONS

1. The amplifier design presented in earlier quarterly reports employed simultaneous cavity resonance of both signal and pump fields within the dielectric cylinder resonator. For dc magnetic fields different from zero, it is necessary for both signal and pump modes to be magnetodynamic, and thus have field dependent resonant frequencies. Magnetic tuning of the amplifier is impossible, however, for the fixed pump frequency available, unless the size of the resonator is varied by repeated machining. An alternative to the above is the cavity resonance of the pump fields. Such has the advantage of allowing Q values larger than those obtainable with dielectric materials available for the present design. Also, the possibilities of obtaining uniform magnetic pump fields throughout the volume of the ferrite is enhanced.

2. Magnetodynamic mode plots for dielectric cylinders containing YIG spheres reveals the following concerning splitting of static modes away from the Walker spectrum. On the low field side of the spectrum modes occur with very large and very low splitting factors. On the high field side, the splitting factors are intermediate to high. Operation of the amplifier on the low field side may thus still allow higher signal and idle and consequently lower pump power required at the expense of higher noise figure.

VI. PROGRAM FOR NEXT QUARTER

The dependence of magnetodynamic mode position in field-frequency coordinates on the dimensions of the cylinder and YIG sphere have been explored for a range of sample dimensions, and of resonator enclosure geometries. By proper choice of sample dimensions for a chosen resonator geometry, conditions may be satisfied for pumping any chosen magnetodynamic modes, at specific points along their locus, with pump and signal frequencies within the ranges allowed by available power supplied. The program for next quarter shall concentrate on operating the parametric ferrite amplifier in a sequence of specifically chosen points of magnetodynamic mode operation; the pump power and noise figure may be compared for the points of operation, and thereby, the merits determined of magnetodynamic mode amplifier operation.

Power shall be used in the 20-30 watt C.W., 31-38 kMc range, and in the 13 KW 5 microseconds pulse, 35.6 - 36.1 kMc range.

Pump resonance in a cavity containing the dielectric cylinder shall be continued, and signal shall be coupled into the YIG sample by means of an iris in the pump cavity.

Finally, the pump power requirements from experiment shall be compared with that calculated for those operating

points proving most advantageous for reducing the pump power required.

VII. IDENTIFICATION OF PERSONNEL

	<u>Title</u>	<u>Hours on Contract</u>
Roy W. Roberts	Project Engineer	77
Lee F. Donaghey	Engineer	512
Bert A. Auld	Consultant	24

Biographies of the above personnel appeared in the previous Quarterly Reports.

Organization

No. of Copies

Commanding General U.S. Army Combat Development Command Attn: CDCMR-E Fort Belvoir, Virginia	1
Commanding Officer U.S. Army Communication & Electronics Combat Development Agency Fort Huachuca, Arizona	1
Hq. Electronic Systems Division Attn: ESAT L.G. Hanscom Field Bedford, Massachusetts	1
Director, Fort Monmouth Office U.S. Army Communication & Electronics Combat Development Agency Fort Monmouth, New Jersey	1
AFSC Scientific/Technical Liaison Office U.S. Army Electronics R & D Laboratory Fort Monmouth, New Jersey	1
Sperry Microwave Electronics Company Division of Sperry Rand Corporation P.O. Box 1828 Clearwater, Florida Attn: Mr. B. Duncan	1
Stanford University W.W. Hansen Laboratories of Physics Attn: Dr. J. Shaw Stanford, California	1
Commanding Officer U.S. Army Electronics R & D Laboratory Attn: SELRA/PEM (Mr. N. Lipetz) Fort Monmouth, New Jersey	1
Microwave Associates, Inc. South Avenue Burlington, Massachusetts Attn: Mr. R. Damon	1

Organization

No. of Copies

Marine Corps Liaison Officer
U.S. Army Electronics R & D Laboratory
Attn: SELRA/LNR
Fort Monmouth, New Jersey 1

Commanding Officer
U.S. Army Electronics R & D Laboratory
Attn: Director of Research
Fort Monmouth, New Jersey 1

Commanding Officer
U.S. Army Electronics R & D Laboratory
Attn: Technical Documents Center
Fort Monmouth, New Jersey 1

Commanding Officer
U.S. Army Electronics R & D Laboratory
Attn: Technical Information Division
(FOR RETRANSMITTAL TO ACCREDITED BRITISH AND
CANADIAN GOVERNMENT REPRESENTATIVES)
Fort Monmouth, New Jersey 3

Commanding Officer
U.S. Army Electronics R & D Laboratory
Attn: SELRA/PR (Mr. Garoff) (1 cy)
SELRA/PR (Mr. Hanley) (1 cy)
SELRA/PRG (Mr. Zinn) (1 cy)
SELRA/PRT (Mr. Kaplan) (1 cy)
Fort Monmouth, New Jersey 4

Commanding Officer
U.S. Army Electronics R & D Laboratory
Attn: Logistics Division (For: SELRA/PRM,
Project Engineer)
Fort Monmouth, New Jersey 1

Commanding Officer
U.S. Army Electronics R & D Laboratory
Attn: SELRA/PRM, Record File Copy
Fort Monmouth, New Jersey 1

Commanding General
U.S. Army Materiel Command
Attn: R & D Directorate
Washington 25, D.C.

Westinghouse Electric Corporation
43 West Front Street
Red Bank, New Jersey
Attn: Dr. R.A. Moore 1

<u>Organization</u>	<u>No. of Copies</u>
Commander Rome Air Development Center Attn: RAALD Griffiss Air Force Base, New York	1
AFSC Scientific/Technical Liaison Office U.S. Naval Air Development Center Johnsville, Pennsylvania	1
Chief of Research and Development Department of the Army Washington 25, D.C.	1
Chief, U.S. Army Security Agency Arlington Hall Station Arlington 12, Virginia	2
Deputy President U.S. Army Security Agency Board Arlington Hall Station Arlington 12, Virginia	1
Commanding Officer U.S. Army Electronics Research Unit P.O. Box 205 Mountain View, California	1
Commanding Officer Harry Diamond Laboratories, Connecticut Ave. & Van Ness St., N.W. Attn: Library, Rm. 211, Bldg. 92 Washington 25, D.C.	1
Commander U.S. Army Missile Command Attn: Technical Library Redstone Arsenal, Alabama	1
Commanding Officer U.S. Army Electronics Command Attn: AMSEL-AD Fort Monmouth, New Jersey	3
Commanding Officer U.S. Army Electronics Materiel Support Agency Attn: SELMS-ADJ Fort Monmouth, New Jersey	1
Corps of Engineers Liaison Office U.S. Army Electronics R & D Laboratory Fort Monmouth, New Jersey	1

Organization

No. of Copies

OASD (R&E)
Attn: Technical Library
Rm. 3E1065, The Pentagon
Washington 25, D.C. 1

Commander
Armed Services Technical Information Agency
Attn: TISIA
Arlington Hall Station
Arlington 12, Virginia 20

Advisory Group on Electron Devices
346 Broadway
New York 13, New York 2

Director
U.S. Naval Research Laboratory
Attn: Code 2027
Washington 25, D.C. 1

Commanding Officer & Director
U.S. Navy Electronics Laboratory
San Diego 52, California 1

Chief, Bureau of Ships
Department of the Navy
Attn: 681A-1
Washington 25, D.C.

Commander
Aeronautical Systems Division
Attn: ASAPRL
Wright Patterson AFB, Ohio 1

Commander, AF Cambridge Research Laboratories
Attn: CCRR (1 cy)
CCSD (1 cy)
CRZC (1 cy)
L.G. Hanscom Field
Bedford, Massachusetts 3

Commander
Air Force Cambridge Research Laboratory
Attn: CRXL-R, Research Laboratory
L.G. Hanscom Field
Bedford, Massachusetts 1

